Molecular filaments and the origin of the IMF

Ph. André[1], V. Könyves[1], D. Arzoumanian[2], and A. Roy[1]

[1] CEA Saclay – Laboratoire d'Astrophysique (AIM), Orme des Merisiers Bât. 709, F-91191 Gif-sur-Yvette, France, e-mail: `pandre@cea.fr`

[2] Department of Physics, Graduate School of Science, Nagoya University, Furo-cho, Chikusa-ku, Nagoya 464-8602, Japan

Abstract. The origin of the IMF is one of the most debated issues in astrophysics. We discuss new insights into this problem since the IMF@50 conference coming from *Herschel* observations. The *Herschel* results point to the key role of the filamentary structure pervading molecular clouds. They suggest that the prestellar cores responsible for the peak of the IMF result from gravitational fragmentation of filaments near the critical line mass.

Key words. Stars: formation – ISM: clouds – ISM: structure, submillimeter

1. Introduction

The origin of the stellar initial mass function (IMF) remains highly debated. Two major features of the IMF are 1) a fairly robust power-law slope at the high-mass end (Salpeter 1955), and 2) a broad peak around $\sim 0.3\,M_\odot$ corresponding to a characteristic stellar mass scale (e.g. Larson 1985). In recent years, the dominant theoretical model proposed to account for these features has been the "gravo-turbulent fragmentation" picture (e.g. Hennebelle & Chabrier 2008), whereby the properties of interstellar turbulence lead to the Salpeter power law and gravity sets the characteristic mass scale. Here, we discuss modifications to this picture based on *Herschel* results in nearby molecular clouds which emphasize the importance of filaments in the star formation process (e.g. André et al. 2010).

Herschel imaging observations demonstrate that molecular filaments are truly ubiquitous and present a high degree of universality. A detailed analysis of the radial column density profiles shows that, at least in the nearby clouds of the Gould Belt, filaments are characterized by a narrow distribution of central widths with a typical FWHM value ~ 0.1 pc and a dispersion of less than a factor of 2 (Arzoumanian et al. 2011). Another major result from *Herschel* (e.g. Könyves et al. 2015, cf. Fig. 1) is that most ($> 75\%$) prestellar cores are found in dense, "supercritical" filaments for which the mass per unit length exceeds the critical line mass of nearly isothermal, long cylinders (e.g. Inutsuka & Miyama 1997), $M_{\text{line,crit}} = 2\,c_{\text{s}}^2/G \sim 16\,M_\odot/\text{pc}$, where $c_{\text{s}} \sim 0.2$ km/s is the isothermal sound speed for molecular gas at $T \sim 10$ K. These findings support a scenario in which low-mass star formation occurs in two main steps (André et al. 2014): First, large-scale compression of interstellar material in supersonic MHD flows generates a cobweb of ~ 0.1-pc-wide filaments in the ISM; second, the densest filaments fragment into prestellar cores (and then protostars) by gravitational instability above the critical line mass $M_{\text{line,crit}}$, corresponding to $\Sigma_{\text{gas}}^{\text{crit}} \sim$
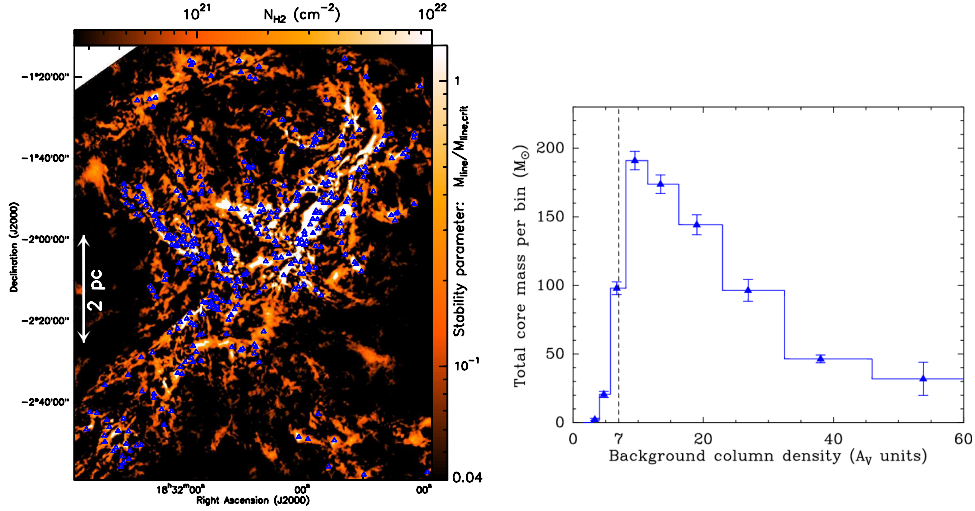
Fig. 1. Left: Column density map of part of the Aquila molecular cloud as derived from *Herschel* data (André et al. 2010; Könyves et al. 2015). The contrast of the filaments has been enhanced using a curvelet transform. The areas where the filaments have a mass per unit length larger than half the critical value $2\,c_s^2/G$ are highlighted in white. The prestellar cores identified by Könyves et al. (2015) are shown as small blue triangles. **Right:** Mass in the form of prestellar cores in the Aquila cloud as a function of background column density in A_V units (based on the results of Könyves et al. 2015). The peak seen at $A_V \sim 10$ implies that most prestellar cores form just above the column density threshold ($A_V^{back} \sim 7$), in marginally supercritical filaments.

$160\,M_\odot/\mathrm{pc}^2$ in gas surface density ($A_V \sim 7.5$ – cf. Fig. 1b).

2. The role of filaments in the IMF

In the filamentary paradigm of star formation emerging from *Herschel* observations, the dense cores making up the peak of the prestellar core mass function (CMF) – likely responsible for the peak of the IMF – result from gravitational fragmentation of filaments near the critical threshold for global gravitational instability. Indeed, the peak of the prestellar CMF at $\sim 0.6\,M_\odot$ as observed in the Aquila cloud complex (Könyves et al. 2015 – cf. Fig. 2a) corresponds very well to the thermal Jeans or Bonnor-Ebert mass $M_{BE} \sim 1.3\,c_s^4/G^2\Sigma_{cl} \sim 0.5\,M_\odot$ within marginally critical filaments of ~ 0.1 pc width with $M_{line} \approx M_{line,crit}$ and $\Sigma_{cl} \approx \Sigma_{gas}^{crit} \sim 160\,M_\odot\,\mathrm{pc}^{-2}$.

Naively, one would expect filament fragmentation to result in a narrow prestellar CMF sharply peaked at the median thermal Jeans mass. However, two effects can contribute to broadening the CMF. First, turbulence generates a field of initial density fluctuations within the filaments (Inutsuka 2001). Based on a study of the density fluctuations observed with *Herschel* along a sample of 80 subcritical or marginally supercritical filaments in three nearby clouds, Roy et al. (2015) found that the power spectrum of line-mass fluctuations is well fit by a power law, $P(k) \propto k^\alpha$ with $\alpha = -1.6 \pm 0.3$. This is consistent with the 1D power spectrum generated by subsonic Kolmogorov turbulence ($\alpha = -5/3$). Starting from such an initial power spectrum, the theoretical analysis by Inutsuka (2001) shows that the density perturbations quickly evolve – in about two free-fall times or ~ 0.5 Myr for a critical 0.1 pc-wide filament – from a mass distribution similar to that of CO clumps to a population of protostellar cores whose mass distribution approaches the Salpeter power law at the high-mass end. Second, star-forming filaments themselves have a broad distribu-
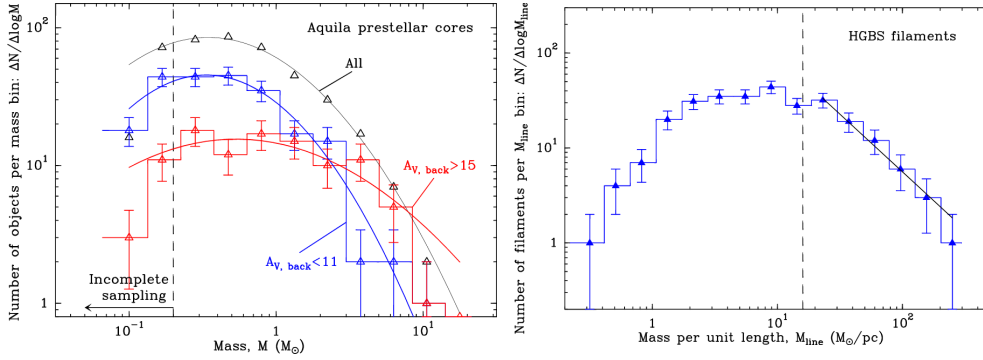
Fig. 2. Left: Prestellar core mass function (dN/dlog$M$) observed with *Herschel* in the Aquila cloud (Könyves et al. 2015). Black triangles: CMF for the whole sample of 446 candidate prestellar cores identified in the cloud. Blue histogram and triangles: CMF observed at low background column densities ($A_V^{back} < 11$). Red histogram and triangles: CMF at high background column densities ($A_V^{back} > 15$). Note how the CMF extends to higher masses at higher background column densities, i.e., higher M_{line} filaments. **Right:** Preliminary distribution of line masses obtained from *Herschel* data for a sample of 278 nearby filaments (Arzoumanian et al., in prep.). Above the critical line mass $M_{line,crit} \sim 16\,M_\odot$/pc, the filament sample is essentially complete and the distribution is well fitted by a Salpeter-like power law dN/dlog$M_{line} \propto M_{line}^{-1.2\pm0.2}$.

tion of masses per unit length (cf. Fig. 2b), which leads to a distribution of characteristic core masses. Given the typical filament width ~ 0.1 pc and the fact that thermally supercritical filaments are observed to be in rough virial balance with $M_{line} \sim M_{line,vir} \equiv 2\,c_{s,eff}^2/G$ where $c_{s,eff}$ is the effective sound speed (Arzoumanian et al. 2013), it is easy to show that the effective Bonnor-Ebert mass $M_{BE,eff} \sim 1.3\,c_{s,eff}^4/G^2\Sigma_{fil}$ scales as M_{line}. Hence, more massive cores may form in higher M_{line} filaments (cf. Fig. 2a), and the Salpeter-like distribution of line masses observed above $M_{line,crit}$ (cf. Fig. 2b) should directly translate into a Salpeter-like power-law distribution of characteristic prestellar core masses (cf. André et al. 2014). Moreover, as shown by Lee et al. (2017), the convolution of the distribution of filament line masses with the CMF produced by individual filaments results in a fully realistic global CMF/IMF.

References

André, Ph., Di Francesco, J., Ward-Thompson, D. et al. 2014, in Protostars and Planets VI, H. Beuther et al. eds. (Univ. of Arizona Press, Tucson), 27

André, Ph., Men'shchikov, A., Bontemps, S., et al. 2010, A&A, 518, L102

Arzoumanian, D., André, Ph., Didelon, P., et al. 2011, A&A, 529, L6

Arzoumanian, D., André, Ph., Peretto, N., Könyves, V. 2013, A&A, 553, A119

Hennebelle, P., & Chabrier, G. 2008, ApJ, 684, 395

Inutsuka, S-I, & Miyama, S.M. 1997, ApJ, 480, 681

Inutsuka, S. 2001, ApJ, 559, L149

Könyves, V., André, Ph., Men'shchikov, A., et al. 2015, A&A, 584, A91

Larson, R.B. 1985, MNRAS, 214, 379

Lee, Y.–N., Hennebelle, P., Chabrier, G. 2017, A&A, submitted

Roy, A., André, Ph., Arzoumanian, D., et al. 2015, A&A, 584, A111

Salpeter, E.E. 1955, ApJ, 121, 161